

# INDIRECT MEASUREMENTS OF ATMOSPHERIC TEMPERATURE PROFILES FROM SATELLITES:

## VI. HIGH-ALTITUDE BALLOON TESTING

D. Q. WARK

National Environmental Satellite Center, ESSA, Washington, D.C.

F. SAIEDY

University of Maryland, College Park, Md.

D. G. JAMES

British Meteorological Office, Bracknell, Berkshire, England

### ABSTRACT

The balloon model of the Satellite Infrared Spectrometer has been flown with balloons at altitudes of about 30 km. from Palestine, Tex. and Sioux Falls, S. Dak. The instrument was calibrated in flight by reference to an internal blackbody at a measured temperature; radiances were deduced for each of the six intervals in the 15- $\mu$  band and the interval at 11.1 $\mu$  in the window. During the Palestine flight the balloon passed over clear areas and over cumulonimbus clouds whose tops were at about 250 mb. From data in each area, the vertical temperature profile was deduced and compared with radiosonde data; in the cloudy areas the profile was limited to the region above the clouds. From data in the 11.1- $\mu$  channel, surface temperatures were deduced; the temperatures, corrected for atmospheric water vapor, were compared with special surface temperature measurements and with screen temperatures from Weather Bureau stations. Because of strong radio frequency interference, the 15- $\mu$  channels of the Sioux Falls flight were of reduced quality and it was possible to retrieve only a few data for the temperature profile; however, the 11.1- $\mu$  data were satisfactory for good surface temperature determination.

### 1. INTRODUCTION

In the preceding papers of this series the theoretical groundwork has been laid for inferring vertical temperature profiles from satellite measurements of spectral radiance in the 15- $\mu$  carbon dioxide band. Theory and instruments have been developed, and measurements have been made from the ground looking upward. These ground-based determinations have serious and fundamental shortcomings, as was evident in the discussions by James [7] and by Wolk, Van Cleef, and Yamamoto [11]. The situation is reversed when the view of the atmosphere is from above. The balloon flights described by Hilleary et al. [5] provide an opportunity to evaluate the ultimate objective, observations from satellites.

In certain ways the balloon observations have clear advantages over satellite observations, but, of course, lack the flexibility and worldwide coverage of the latter, and have no reason for existing in themselves. However, by

the small area of view, concurrent photographs of high quality, measurements of surface and soil temperatures at the ground, the presence of several nearby radiosonde stations conducting special ascents, short-range telemetry, uniquely favorable transmittance functions in certain channels, and other specially contrived measurements and conditions, the balloon tests are highly controlled experiments which test both the instrument and the ability to retrieve temperature profiles from measurements of high quality.

As already mentioned by Hilleary et al. [5], the performance of the instrument was not flawless during the first flight, and strong radio-frequency interference bothered the second flight. Far from indicating failure, however, these flights were triumphs in revealing hidden possibilities of failure of a satellite instrument and therefore contributed strongly to anticipated success in that ultimate experiment. From the standpoint of useful radiance data, it was necessary to discard those from one

channel from the first flight; from the second flight a few sets of data were retrieved by J. H. Lienesch and S. D. Soules after a lengthy examination of the record.

These balloon flights introduced another measurement by the spectrometer which has barely been mentioned heretofore: the 9-cm.<sup>-1</sup> channel centered at 899 cm.<sup>-1</sup>, a region of the optical window lying between water vapor absorption lines and affected only by the quasi-continuum, which has its minimum absorption in this vicinity. The purpose of this channel is to aid in the determination of pressure altitudes of clouds, which affect the radiances in some of the channels in the 15- $\mu$  carbon dioxide band. From the altitudes of the balloons, however, the area of view was small enough to allow one to measure the radiance temperature of the surface during long periods of the flights. A separate analysis has been made of the output of this channel, which performed well during both flights.

## 2. CALIBRATION

As shown in other papers of this series, the relative values of the radiances in the intervals in the 15- $\mu$  carbon dioxide band are of critical importance in recovering the temperature soundings. The greatest care must therefore be observed in calibrating the instrument in order to recover radiances which meet the stringent requirements of the experiment.

It is not possible to obtain a simple and final calibration of the instrument's response because the gain of the amplifiers is a function of the internal temperature of the instrument, and because changes may occur after the ground calibration. Therefore, an in-flight calibration is needed. This is achieved by occasionally, upon command from the ground, directing the field of view toward the reference cone blackbody, whose temperature is measured.

The reference source consists of a copper cone painted on the inside with a black paint of high emissivity (about 0.98); as mentioned by Hilleary et al. [5], the emissivity of such a cone is in excess of 0.99. On comparison of the reference cone against laboratory blackbodies it was found that the radiation from each was within the root mean square error [0.3 erg/(sec. cm.<sup>2</sup> strdn. cm.<sup>-1</sup>)] of the instrumental measurements. The temperature of the reference cone is determined by the measurement of the voltage across a thermistor bead in a simple circuit; this voltage is calibrated against a precision thermocouple.

The amplifiers of the instrument were designed to be linear. However, as a further check the linearity of the instrument was determined in the laboratory by means of a blackbody whose temperature was varied over a wide range. During this test the temperature of the instrument was kept nearly constant (25°–30° C.), so that the gains of the amplifiers were constant. It was found from this test that the instrument is indeed linear within its noise figure.

Because the response of the instrument is linear, the radiance of the source measured in each channel,  $i$ , can be represented by

$$I_i = m_i (V_i - v_i), \quad i=1, \dots, 7 \quad (1)$$

where

$$I_i = \text{Radiance in erg/(cm.}^2 \text{ sec. strdn. cm.}^{-1})$$

$$m_i = \text{Slope of the calibration in erg/(cm.}^2 \text{ sec. strdn. cm.}^{-1}) \text{ per volt}$$

$$V_i = \text{Output voltage}$$

$$v_i = \text{Electronic zero (the voltage output of the instrument for zero source radiance).}$$

The in-flight calibration is accomplished by first blocking the chopped beam to determine  $v_i$ . The reference cone is then placed in position to fill the field of view of the instrument (earth port); the outputs of the instrument correspond to the spectral radiances of the reference cone, whose temperature is reported continuously. Hence the slopes of the calibrations ( $m_i$ ) of the instrument can be obtained.

For the six carbon dioxide channels this procedure is complicated by the fact that there are three ranges (described by Hilleary et al. [5]). Normal operation during the flight is on mid-range because the mean radiative temperature of the channels in the carbon dioxide band is around 230° K., while the reference cone temperature is sufficiently high (288° K.) to put it on the high range. It is thus necessary to know not only the slopes,  $m_i$ , but also the voltage offsets,  $v_{ij}$ , for the mid- and high-range channels.

The data from the pre-flight and post-flight calibrations made with external blackbody sources in the two beams of the instrument were linear everywhere but near zero radiance. The non-linearities are attributed to the differences in the two blackbody sources, mainly in the exact determination of the temperatures of their radiating surfaces.

When the calibration data in the non-linear region are eliminated, a least-squares fit can be made to the remaining data for the slopes,  $m_i$ , and the voltage intercepts,  $(v_{ij} + v_i)$ . In a perfectly linear calibration, the regression should pass through the origin ( $v_{ij} + v_i = 0$ ), but it is found to be displaced systematically. The intercepts,  $(v_{ij} + v_i)$ , must then be subtracted from all voltages, so that the radiances are now given by

$$I_i = m_i [(V_i - v_i) + (v_{ij} - v_{ij})], \quad i=1, \dots, 7, \quad j=1, 2, 3. \quad (2)$$

TABLE 1.—Slopes and intercepts (voltage offsets) derived from the ground calibrations for the Palestine flight

Channel (i)	$v_i$ (cm. <sup>-1</sup> )	$m_i$ [erg/(cm. <sup>2</sup> sec. strdn. cm. <sup>-1</sup> ) per volt]	Intercepts (voltage offsets)	
			$v_{i2} - v_{i1}$	$v_{i3} - v_{i1}$
A (1)	669.0	11.914	2.026	8.028
B (2)	677.5	10.738	2.003	7.849
C (3)	691.0	11.710	2.000	7.846
D (4)	697.0	11.574	2.000	7.934
E (5)	703.0	11.714	2.006	7.817
F (6)	709.0	11.469	2.002	7.798
G (7)	899.0	30.04	0	0

The slopes and the intercepts (voltage offsets for the medium and high ranges),  $m_i$  and  $(v_{i2}-v_{i1})$ , are given in table 1 for the ground calibration of the Palestine flight. Because channel G has only one range,  $(v_{72}-v_{71}) = (v_{73}-v_{71}) \equiv 0$ .

The voltages,  $V_i$ , were measured during the flight, and the zero-radiance voltages,  $v_i$ , were measured during the in-flight calibrations. Thus, the first parenthetic term on the right in equation (2) is the observed quantity, and the second term is the constant offset voltage. The voltage offsets are independent of the temperature of the instrument and are produced by a highly stabilized power supply, and their values were checked during flight by the introduction of a false signal. The slopes,  $m_i$ , are dependent upon the temperature of the instrument, and were re-determined from the flight calibration data; during the flight the temperature was about 15°-19° C., whereas it had been 25°-30° C. during the ground calibrations.

A full description of the telemetry calibration is given by Hilleary et al. [5]. For an input of 0 to 5 volts the telemetry encoder produces a 3-digit number between 999 and 000. The conversion is linear within this range but is not the same for each of the channels. The encoder calibration for each of the channels was determined experimentally during one of the routine general calibrations and a straight line fitted for each set of points by the least squares method.

During the calibration sequence the output of the instrument recorded in turn:

- (1) Electronic zero,  $v_i$ , in which the chopped beam was blocked.
- (2) False signal when known voltages were applied to the amplifiers,  $(v_{i2}-v_{i1})$  and  $(v_{i3}-v_{i1})$ .
- (3) Voltages from the reference cone,  $V_i$ , from which the radiances,  $I_i$ , were calculated from the Planck relation
- (4) The transmittance of a calibration filter which was inserted before the reference cone so that the wavelength calibration could be checked.

Each of the above parameters was examined for about a minute. The temperature of the reference cone was reported continuously on a separate channel of the telemetry system. These measurements were used for the instrument calibration as described above. The slopes,  $m_i$ , of the

calibration changed during the Palestine flight by only 1.2 percent, and linear interpolation with time was sufficiently accurate.

After the Palestine flight the recovered instrument, upon return to the laboratory, was found to be in good working order. Post-flight calibration and preliminary inspection of the flight data revealed that channels A and B might have suffered electronic malfunctioning. This caused a re-assessment of both in-flight and ground calibration for these channels. However, by the use of a more complicated calibration procedure it was possible to obtain meaningful radiances in channel B with accuracies compatible to those of channels C-G. For channel A the uncertainty could not be removed and therefore this channel was excluded from our computation.

Following the calibration procedure described, the radiances in the channels were computed every 15 sec., except for those periods when the instrument was in a calibration sequence. Table 2 presents three sample sets of data, two for clear conditions and the third for a completely overcast case.

For the Sioux Falls flight the calibration procedure was essentially the same as that followed for the Palestine flight. However, because of the strong radio interference it was necessary to use the pre-flight and post-flight calibration data; the few in-flight data which could be

TABLE 2.—Calculated and observed radiances,  $I_T^c$  and  $I_T^o$ , for the two balloon flights. Values are in  $\text{erg}/(\text{cm}^2 \text{ sec. strdn. cm.}^{-2})$ , and the subscript  $T$  is time, *cst*. The radiances and times for the Sioux Falls observation are the means of six

Channel	$v_i$ ( $\text{cm.}^{-1}$ )	Palestine, clear			Palestine, cloudy		Sioux Falls	
		$I_{1200}^c$	$I_{0757}^o$	$I_{1502}^o$	$I_{1200}^c$	$I_{1217}^o$	$I_{1200}^c$	$I_{1222}^o$
A	669.0							
B	677.5	42.4	41.3	42.3	42.3	42.1	45.5	44.4
C	691.0	39.6	40.1	40.1	39.4	38.9	44.0	44.1
D	697.0	42.7	43.7	43.2	40.6	40.0	44.0	44.4
E	703.0	51.8	52.2	51.7	43.2	42.8	47.1	49.0
F	709.0	63.2	65.0	64.3	44.9	45.1	53.6	55.4
G	899.0	122.3	110.4	>132	30.6	30.6	77.5	77.5

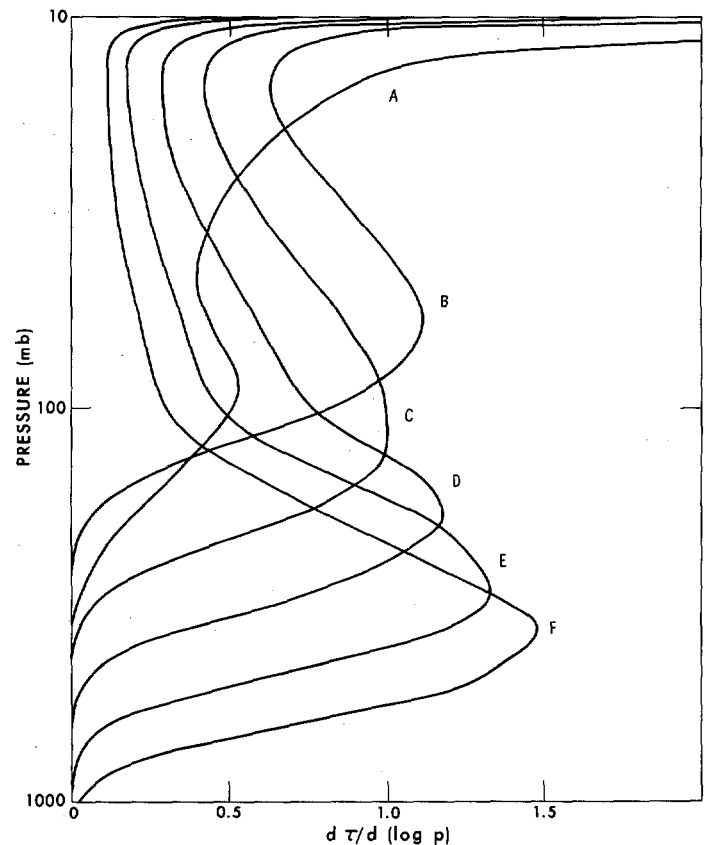


FIGURE 1.—The transmittance weighting functions of the six carbon dioxide intervals calculated from the 1200 *cst*, September 11, 1964, Fort Worth temperature and humidity profiles.

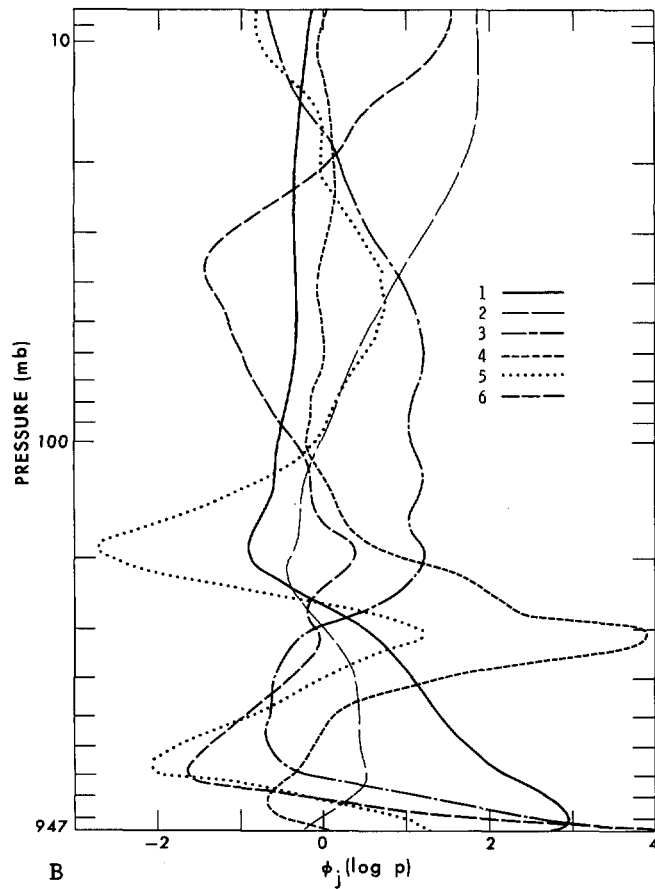
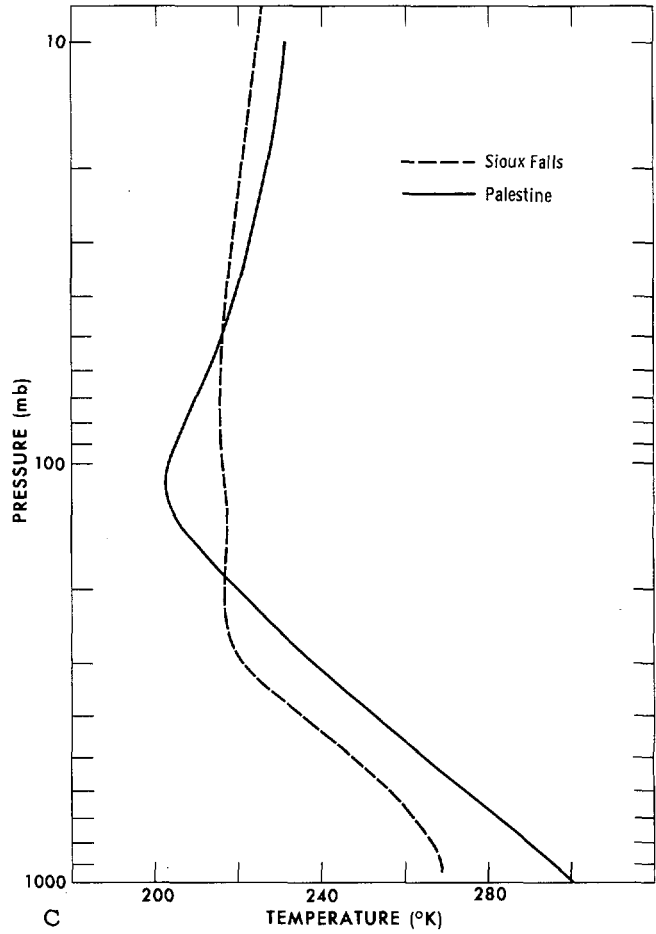
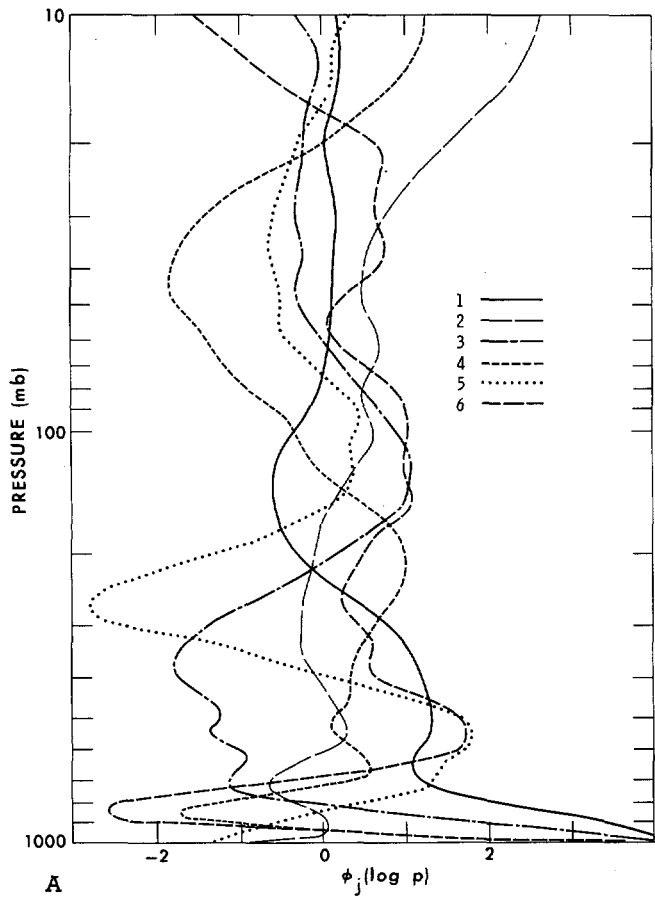


FIGURE 2.—Empirical orthogonal functions derived from (a) 90 Fort Worth soundings and (b) 96 St. Cloud and Omaha soundings; (c) shows the associated mean temperature profiles (solid and dashed, respectively).

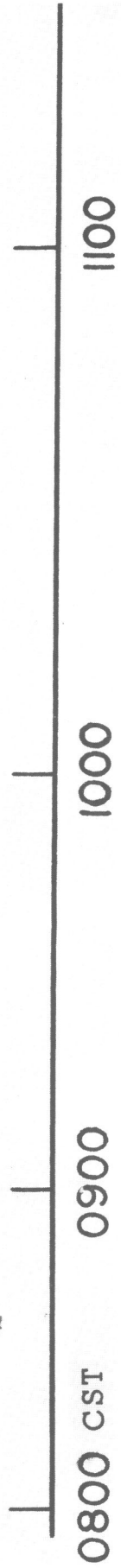




FIGURE 3.—Mosaic of photographs taken from the balloon during the Palestine flight. The view is vertical, and the camera was aligned with the spectrometer, whose field of view has about half the dimensions of a single photograph. Note overlap providing continuity between consecutive panels where mosaic had to be cut.

relied upon were used only as validations. From about a thousand sets of radiance data only six showed a degree of stability which suggested they might be used to deduce the temperature profile. Data from the poorest channel showed variations of as much as 30 percent during a 15-sec. observation period (the telemetry system on this flight was a continuous-reading analog signal); other channels were better, but their telemetered data did not represent the quality of the instrument. It is quite probable that the errors of the few data recovered are substantially larger than those of the Palestine flight; their quality is systematic, rather than random. These data are presented in table 2.

### 3. TEMPERATURE PROFILES

The procedures for retrieval of temperature profiles have been discussed by Wark and Fleming [10] in the first paper of this series. It consists of the solution of the set of equations,

$$g(\nu_i) = \frac{I(\nu_i) - \beta(\nu_i)}{\alpha(\nu_i)} + \int_1^0 \overline{B(\nu_i, t)} d[\tau(\nu_i, t)] \\ = - \sum_{j=1}^N c_j \int_1^0 \phi_j(t) d[\tau(\nu_i, t)], \\ i=1, \dots, N, \quad j=1, \dots, N \quad (3)$$

for the set of coefficients  $c_j$ ; definitions of the terms are contained in Wark and Fleming [10] and Alishouse et al. [1]. The minimization technique described in the first of these papers is applied to equation (3), where the  $\phi_j(t)$  are empirical orthogonal functions described in the latter paper. The independent variable  $t$  is a function of the atmospheric pressure,  $p$ ; it has been found convenient to use  $t = \log p$ .

Although the solution for the temperature profiles follows the procedures already established, the fractional transmittances  $\tau(\nu_i, t)$  differ substantially in the balloon case from the satellite case. This is particularly true near the balloon level, where significant absorption by carbon dioxide takes place near the band center. The first procedure is therefore a determination of the transmittance functions from calculations and laboratory data.

The transmittance in each interval was approximated in the same way as in the previous paper,

$$\tau(\nu_i, t) = \tau_{\text{CO}_2}(\nu_i, t) \cdot \tau_{\text{H}_2\text{O}}^1(\nu_i, t) \cdot \tau_{\text{H}_2\text{O}}^{\text{c}}(\nu_i, t), \quad (4)$$

where the terms on the right are the transmittances by carbon dioxide, water vapor lines, and the water vapor quasi-continuum. The carbon dioxide transmittances were calculated for a random Elsasser band model, with the Curtis-Godson approximation (see Wark [9]); line strengths and widths were adjusted to fit recent laboratory measurements. In the Q-branch interval the transmittance was found from special laboratory measurements by M. Wolk. The water vapor transmittances were calculated from a random model (Goody [4], Godson [3]), weighted

by the slit function of the instrument; absorption coefficients for the quasi-continuum were taken from Saeidy [8].

The water vapor distribution was obtained from nearby radiosonde data. Of course, the contribution to the transmittances by water vapor is negligible except in the lower troposphere (below about 500 mb. at Palestine, where the humid air contained 5 cm. of precipitable water vapor; and nearly to the surface at Sioux Falls, where the dry air contained only 0.5 cm. of precipitable water vapor).

Figure 1 shows the transmittance weighting functions  $d[\tau(\nu_i, \log p)]/d(\log p)$  for the Palestine flight; similar functions for Sioux Falls are almost identical, differing only in the effects of water vapor, temperature, and the pressure altitude of the balloon. Channel A is included, although it is not used with the Palestine data. The transmittances were determined for the known temperature profile, inasmuch as it is not within the scope of this discussion to undertake the iterative procedure for temperature corrections to the transmittances which are to be used later with satellite data; although the iteration is almost trivial, the body of data required in its execution has not yet been calculated.

As discussed in Alishouse et al. [1], the optimal empirical orthogonal functions to be used in the solution are those based upon radiosondes expressing the climatology of the location and the season. A sample of 90 soundings by radiosondes from Fort Worth, Tex. for the months of August and September during several years were used to develop a set of empirical functions for analysis of the Palestine data; only soundings by radiosondes reaching to 25 mb. were used, and they were either extrapolated to 10 mb. or truncated at 10 mb., depending on the maximum altitude. The same procedure was used with a sample of 96 soundings by radiosondes from St. Cloud, Minn. and Omaha, Nebr. for the months of February and March in developing the empirical functions for use with the Sioux Falls data; the limiting pressure was 8.2 mb. in this sample.

By the method of Holmström [6], discussed by Alishouse et al. [1], the first six empirical orthogonal functions were calculated from each sample. Those for Palestine and Sioux Falls are shown in figures 2a and 2b; the associated mean temperature profiles are shown in figure 2c. A maximum of five functions can be used with the Palestine data, and six functions with the Sioux Falls data.

The photographs taken from the balloons are important adjuncts to the interpretation of data, inasmuch as the clouds contribute to the radiances in the more transparent channels. Figure 3 is a photographic strip mosaic of the area below the balloon during the Palestine flight. During the morning the balloon passed over areas largely devoid of clouds. At noon it passed over cumulonimbus clouds for about 40 min. During the latter part of the flight the clouds were of decreasing vertical extent, and there was a cloudless area at the termination of the flight in mid-afternoon. The area viewed by the spectrometer had dimensions about half those of the individual photographs composing figure 3.

The sky was almost entirely clear during the Sioux Falls flight, and the photographs are therefore omitted.

In cloudless areas the solution of equation (3) to determine the temperature profiles is direct, inasmuch as the transmittances are zero at the surface for all the carbon dioxide channels. If clouds exist at levels where the transmittances in any of the carbon dioxide channels are not zero, the limits of the two integrals in equation (3) are from unity to the transmittance at the cloud level,  $\tau(\nu_i, t_c)$ , where the subscript  $c$  refers to the cloud. Then (3) must be rewritten.

$$g(\nu_i) = \frac{I(\nu_i) - \beta(\nu_i)}{\alpha(\nu_i)} + \int_1^{\tau(\nu_i, t_c)} B(\nu_r, t) d[\tau(\nu_i, t)] - B[\nu_r, t_c] \tau(\nu_i, t_c) \\ = - \sum_{j=1}^N c_j \int_1^{\tau(\nu_i, t_c)} \phi_j(t) d[\tau(\nu_i, t)]. \quad (5)$$

It is at this point that the 899  $\text{cm.}^{-1}$  channel becomes vital;  $B[899, T(t_c)]$  can be transformed to  $B[\nu_r, T(t_c)]$ .

The procedure now becomes iterative, inasmuch as  $t_c$  (i.e., the pressure level of the cloud top) is unknown. After an initial guess at  $t_c$ , equation (5) is solved to obtain the temperature sounding. By repeated guesses at  $t_c$ , a value can quickly be found for which the temperature sounding value at the cloud can be made to agree with the temperature found from the 899- $\text{cm.}^{-1}$  channel. One may ignore the absorption by water vapor in this channel because the amount of that gas is normally very small above clouds, and the lower pressure reduces even the effect of this.

From radiosonde data obtained at Fort Worth and at stations near Sioux Falls, equations (3) and (5) were used to calculate the "exact" radiances which were to be expected during the Palestine and Sioux Falls flights. The values are given in table 2.

Results of the analyses of data from the two balloon flights are presented in figures 4 and 5. Figures 4a through 4c show, in order, the derived soundings for the clear area at 7:57 a.m. CST, over the cumulonimbus at 12:17 p.m. CST, and over the second clear area at 3:02 p.m. CST. The dashed curve is the 1800 GMT (noon CST) radiosonde from Fort Worth; comparison of this sounding with others taken at the same time shows the air mass to be essentially uniform over Texas.

Figure 5 is a derived sounding for the Sioux Falls flight taken from the average of six sets of data between 9:52 a.m. and 2:52 p.m. CST. The dashed curve is a noon CST profile at the location of the balloon, as obtained by interpolation from soundings at nearby radiosonde stations.

Figures 4 and 5 reveal significant differences between the profiles taken from radiosonde data and those derived from the spectral radiances. The results from Palestine are superior in some respects to the sounding derived from the Sioux Falls measurements, as was to be expected in view of the radio interference experienced during the latter flight. However, the Palestine results do not meet the standards set by the authors, particularly between 50 and 200 mb. and they are not quite competitive with the radio-

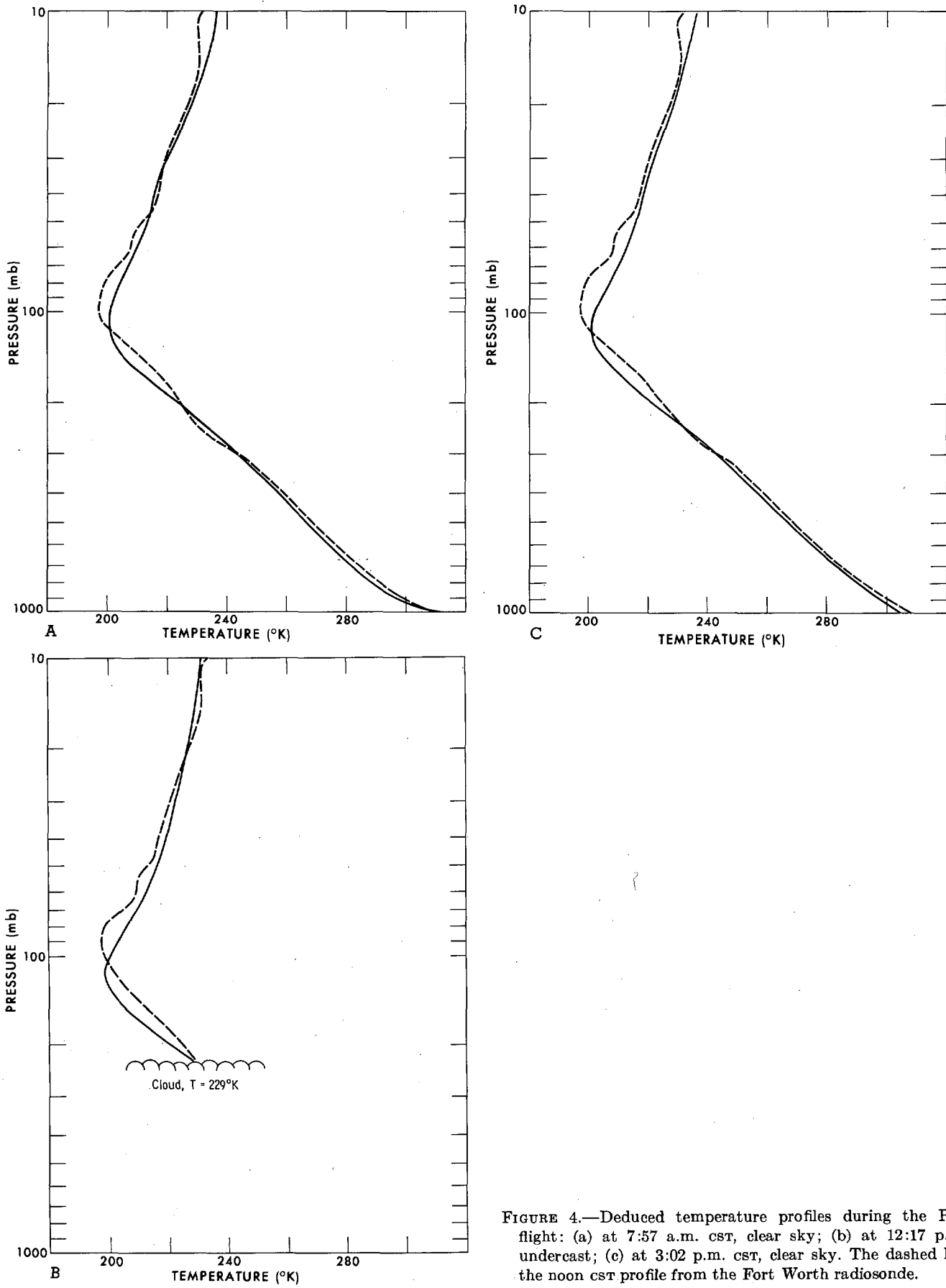


FIGURE 4.—Deduced temperature profiles during the Palestine flight: (a) at 7:57 a.m. CST, clear sky; (b) at 12:17 p.m. CST, undercast; (c) at 3:02 p.m. CST, clear sky. The dashed lines are the noon CST profile from the Fort Worth radiosonde.

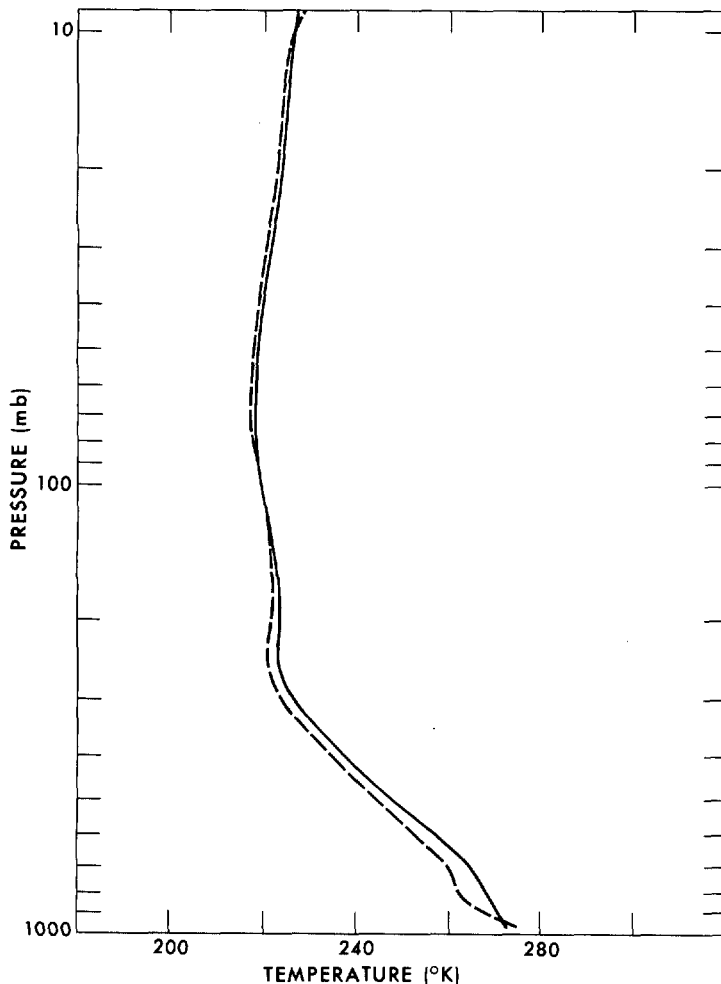


FIGURE 5.—Deduced temperature profile from data of the Sioux Falls flight. The dashed curve is the noon CSR profile interpolated from surrounding radiosondes.

sonde. Possible sources of the differences are:

- (1) The quality of the measurements, including the calibrations and the effects of temperature upon the components of the instrument.
- (2) Incorrect transmittances.
- (3) The basic methods of inversion of the radiative transfer integral equation.
- (4) The application of empirical orthogonal functions in the solutions.

One may quickly dispose of the first two items by calculating the profile from the calculated radiances for the Palestine clear case given in table 2. This profile is found to be insignificantly different from those shown in figures 4a and 4c. The mean deviation of the calculated profile from the Fort Worth sounding is  $1.6^{\circ}$  C. above the 700-mb. level, against  $2.0^{\circ}$  C. from the observed data; the deviations, as seen in figure 4, are mainly near the tropopause and near the balloon (this latter is caused by the missing channel A). Therefore, the differences between calculated and observed radiances given in table 2 for Palestine do not affect the profiles in a significant way. The small

changes in temperature of the instrument during the flight (about  $3^{\circ}$  C.) have been considered in the calibrations, and cannot have any significant influence. It is known that there may be minor errors in the transmittances, manifest mostly in channel F, but the profile derived from the calculated radiances would rule out this cause.

Item 3 may be eliminated by the simple expedient of employing connected line segments for the solution. When this is done, with either calculated or observed radiances, the profiles can be reproduced more reliably, with mean deviations from the Fort Worth sounding of less than  $1^{\circ}$  C.; the region near the tropopause can be made to appear much more accurate. This method of solution, however, is seriously deficient in that it requires that the pressure levels of the terminal points of the line segments be known; this a priori knowledge is not available, and it is difficult to deduce from the data.

Item 4, the empirical functions, is almost totally responsible for the unacceptably large deviations. This becomes apparent from figures 2 and 4. Near the tropopause the deduced profiles for Palestine are remarkably like the mean profile of figure 2c. In figure 2a the empirical functions are seen to be, as a group, smaller in the tropopause region than in the upper and lower parts. In order to obtain the best fit over the entire profile, the coefficients  $c_j$  in equations (3) and (5) must remain small and commensurate with the ensemble of elements of the matrix A (see [10]).

It is apparent that the atmosphere over Texas was anomalous near the tropopause *with respect to the set of radiosonde soundings used to develop the empirical functions*, and a correct solution becomes impossible. The cure for this deficiency is simple in principle, but requires a considerable effort. The sample set of soundings must be chosen to include soundings lying between extremes at every level, *and given equal weights*.

The solution for the undercast condition at Palestine demonstrates the stability at levels where a solution is possible.

The profile for the Sioux Falls flight is, of course, of reduced quality, but has a mean deviation from the radiosonde profile of only  $2.4^{\circ}$  K. above the 700-mb. level. This is better than one might expect from random errors, but table 2 shows the differences between the calculated and observed radiances to be systematic. It is conjectured that this may result from the distances of the individual detectors from the ground bus at channel D. The regression of the radiance differences with wave number has a root mean square deviation of  $0.3 \text{ erg}/(\text{cm}^2 \text{ sec. strdn. cm.}^{-1})$ . This number is in agreement with the noise figure found in laboratory measurements. Although it is somewhat fortuitous, this has the effect of rotating the profile in a uniform fashion, with the major effect in the troposphere, where the kernel functions of figure 3 have their major orthogonal components.

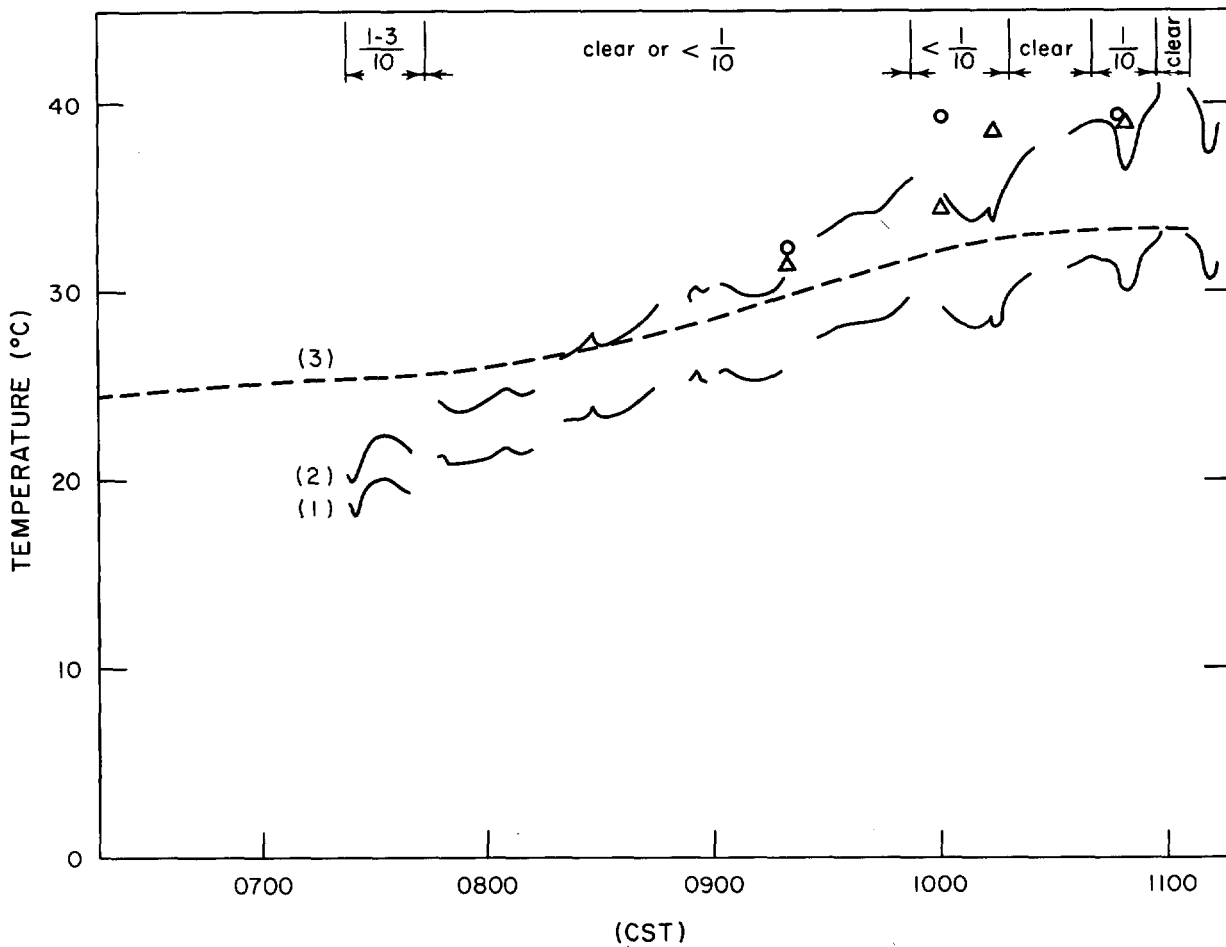


FIGURE 6.—Surface temperature measurements from the Palestine flight. Curve (1) is the temperature equivalent to the measured radiances; curve (2) is surface temperature deduced from the measured radiances; curve (3) is the screen temperature under the balloon; and the symbols ⊙ and Δ are surface temperatures measured under the balloon by a thermistor and a radiometer, respectively.

4. GROUND AND CLOUD TOP TEMPERATURES

The window region at 899 cm.<sup>-1</sup> is by no means completely transparent (see Bignell et al. [2]) because of the quasi-continuum caused by the wings of distant strong water vapor lines. Therefore the emission of the underlying surface is modified by the intervening atmosphere. The measured radiance at the balloon altitude for a uniform field of view is given by

$$I = B(t_c)\tau(t_c) - \int_1^{\tau(t_c)} B(t)d[\tau(t)], \tag{6}$$

where the subscript *c* may be either a cloud or the surface in cloudy or clear conditions; the single wave number  $\nu = 899 \text{ cm.}^{-1}$  is implicit in equation (6).

Because the spectral interval lies between absorption lines, the transmittance from the balloon to any pressure level is given by

$$\tau(p) = \exp\left(-\frac{1}{g} \int_{p_0}^p k \frac{p}{p_0} q dp\right), \tag{7}$$

where *g* is the acceleration of gravity, *k* is the mass absorp-

tion coefficient, the subscripts *b* and 0 refer to the balloon and standard ( $p_0 = 1013 \text{ mb.}$ ) conditions, and *q* is the water vapor mixing ratio. The value of  $k = 0.0925 \text{ cm.}^2/\text{gm.}$  is taken from Saiedy [8].

Equation (6) can be written

$$B(t_c) = \frac{I + \int_1^{\tau(t_c)} B(t)d[\tau(t)]}{\tau(t_c)}. \tag{8}$$

The integral on the right-hand side is the emission contribution by the atmosphere and the denominator is the atmospheric transmittance to the ground or the cloud; both of these factors can be obtained from radiosonde data. Thus, the Planck radiance on the left in equation (8) is computed from the measured radiance, *I*, and the radiative temperature of the cloud or surface is inferred from the Planck equation. If the surface emissivity is assumed to be 1.0, this is the surface temperature, *T<sub>s</sub>*. The values of the surface temperature *T<sub>s</sub>*, computed from the measured radiances and the radiosonde humidity and temperature data at Fort Worth, are given in figure 6 for the early portion of the Palestine flight. This figure

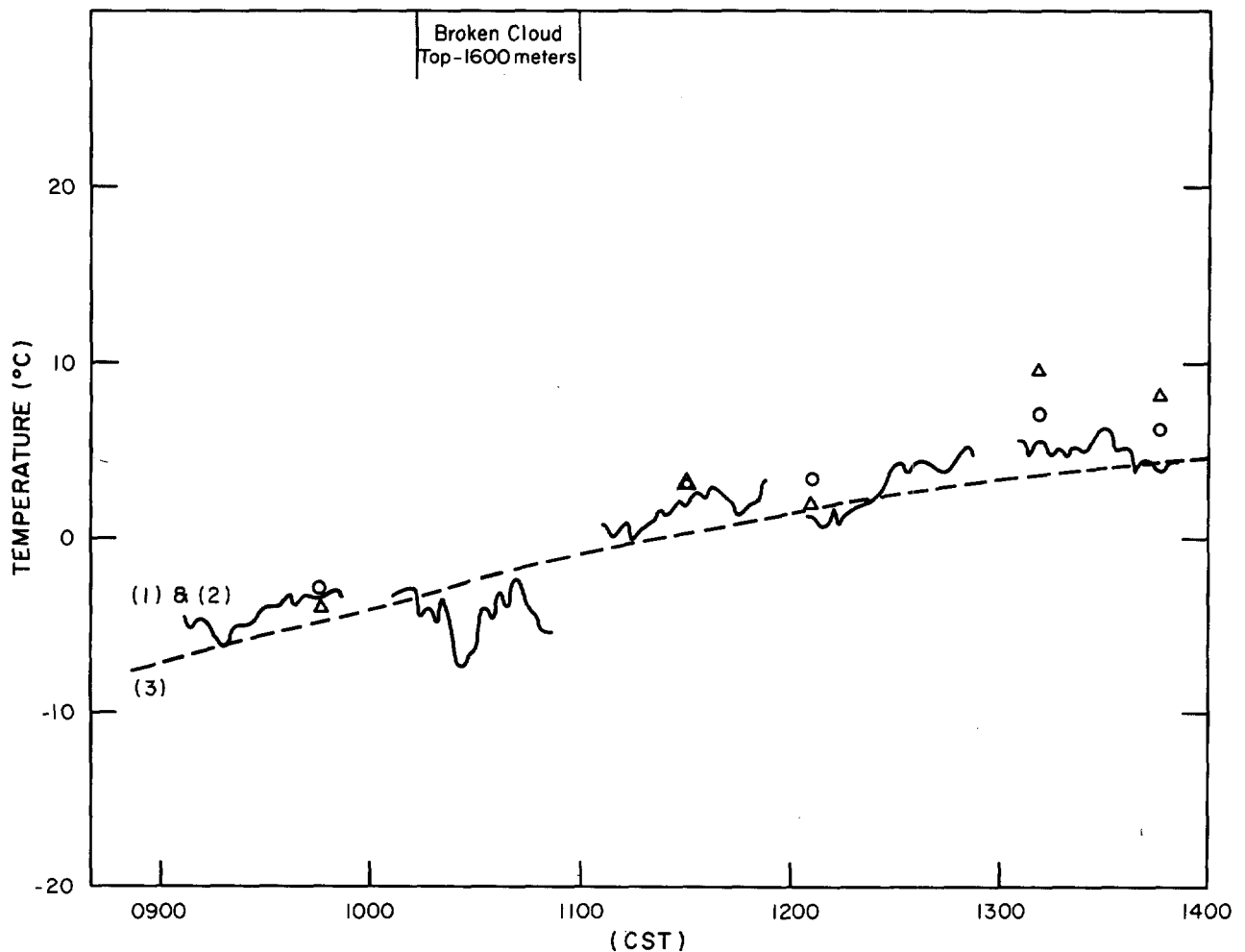


FIGURE 7.—Surface temperature measurements from the Sioux Falls flight. All temperatures are depicted as in figure 6; curves (1) and (2) coincide because of the transparency of the atmosphere.

also includes temperatures equivalent to the uncorrected radiance measurements ( $I(899) = B[899, T(t_e)]$ ).

The surface temperatures were also measured by two different methods at representative sites below the balloon. The first method employed a Stoll-Hardy radiometer, and the second a thermistor bead placed a few millimeters above the surface. The radiometer was calibrated to an accuracy of  $0.5^\circ\text{C}$ . Measurements of the radiometer and the thermistor bead, together with the screen temperature under the balloon as deduced from high density maps of hourly observations, are shown in figure 6.

The surface temperature early in the morning, as deduced from the spectrometer measurements, was  $3^\circ\text{--}4^\circ\text{C}$ . below the screen temperature, indicating a temperature inversion near the ground. From an examination of the Fort Worth radiosonde ascent at 1200 GMT (6:00 a.m. CST), a temperature inversion was found to exist below 953 mb. Later in the day the surface temperature was  $7^\circ\text{C}$ . or more higher than the screen temperature. This is to be expected from the solar heating of the surface on clear mornings, as was the case on the day of the flight.

The fact that the temperature inversion in the morning

and the surface discontinuity near noon have been detected by the radiation measurements points strongly to the correct absolute values of these radiance measurements.

As was mentioned before, the balloon passed over a well-developed storm. The cloud top was extensive enough to fill the field of view of the instrument for 40 min. During this time the measured radiances corresponded to the emission temperatures of the cloud top; the contribution to the measured radiances by the water vapor above the cloud is completely negligible, so that  $I(899) = B[899, T(t_e)]$  is essentially exact. The lowest radiance measured during this time was  $30.6 \text{ erg}/(\text{cm}^2 \text{ sec. strdn. cm.}^{-1})$ , corresponding to a cloud top temperature of  $-44.2^\circ\text{C}$ . ( $229^\circ\text{K}$ ). From the Fort Worth radiosonde data at noon (1800 GMT), the pressure altitude of the cloud was found to be 235 mb.

The results from the Sioux Falls flight are shown in figure 7. The temperatures equivalent to the uncorrected radiance measurements are given; the atmosphere on the day of the flight was essentially transparent because of very low water vapor content, and the correction was

therefore negligible. The surface temperature measurement by the Stoll-Hardy radiometer and the thermistor bead under the balloon are also included in the figure.

The error in the surface temperature measurements is estimated to be  $\pm 0.6^\circ$  C. for the Palestine flight, and approximately double this figure for the Sioux Falls flight. The cause of the reduced accuracy in the Sioux Falls measurement was explained earlier.

## 5. CONCLUSION

This series of six papers has shown the development of a concept for the determination of the three-dimensional temperature field of the atmosphere from radiometric measurements by a satellite. The first two discussed the theoretical concepts, and the third described an instrument developed to obtain the required high quality of measurements. The last three are analyses of measurements made from the ground and from balloons.

The fourth of the series demonstrated that under the most adverse theoretical conditions some information on temperature structure can be obtained from the ground; the quality of the results, however, makes them of doubtful meteorological use. The fifth paper extended the concept of measurements from the ground by increasing the spectral range in the hope of overcoming the deficiencies of the previous study; although the results were improved, they emphasized the perilous path which the employment of this technique from the ground might entail.

The results from the balloon proved, as expected, to be vastly superior. It would be gratifying to report that the results were an unqualified success. It has been shown, however, that a combination of instrumental problems and some unresolved theoretical obstacles have led to retrieved profiles which did not bear out the high promise evidenced in the first paper. The authors, however, have been rewarded with an insight into the specific matters requiring attention in order to achieve a successful program.

The spectrometer has been further developed for eventual use on a satellite. The lessons learned from the balloon flights have been valuable aids in pointing out specific trouble areas, and, to an even greater extent, placing more rigid demands on all aspects of the reliability and quality of the satellite instrument.

This paper has alerted the authors to the pitfalls which may be anticipated in the indiscriminating use of empirical functions derived from randomly selected sets of soundings. A careful examination of the set used for the analysis of the Palestine flight revealed that not one sounding had the characteristics near the tropopause of the Fort Worth sounding of the day of the balloon flight. This, combined with excessive redundancy, led to the empirical functions of figure 2a.

Schemes are now being devised to select sets of sound-

ings which are both representative of geographical location and season, and which are general enough to permit the reproduction of normal and anomalistic soundings. This, and a discussion of solutions for cloud conditions other than thick overcast, will be the subject of future publications.

The discussion of cloud-top and surface temperature measurement given in this paper has been a valuable exposition of the inferences which may be drawn from the use of this narrow window. When the spectrometer is viewing from a satellite, however, the field of view ( $12^\circ$  total angle) will preclude extensive surface measurement with this instrument except in cloudless areas. One may speculate that improved detectors may eventually permit both high spectral and high spatial resolution to exploit the advantage of this narrow window at  $899\text{ cm}^{-1}$ .

Nevertheless, the window measurement is a vital part of the temperature profile determination. It acts as a control, as demonstrated in the cloudy case at Palestine. This control also acts for clear skies and for partly cloudy skies, as will be shown in a later document.

## REFERENCES

1. J. C. Alishouse, L. J. Crone, H. E. Fleming, F. L. Van Cleef, and D. Q. Wark, "A Discussion of Empirical Orthogonal Functions and Their Application to Vertical Temperature Profiles," *Tellus*, in press, 1967.
2. K. Bignell, F. Saiedy, and P. A. Sheppard, "On the Atmospheric Infrared Continuum," *Journal of the Optical Society of America*, vol. 53, No. 4, Apr. 1963, pp. 466-479.
3. W. L. Godson, "The Computation of Infrared Transmission by Atmospheric Water Vapor," *Journal of Meteorology*, vol. 12, No. 3, June 1955, pp. 272-284.
4. R. M. Goody, "A Statistical Model for Water-vapour Absorption," *Quarterly Journal of the Royal Meteorological Society*, vol. 78, No. 336, Apr. 1952, pp. 165-169.
5. D. T. Hilleary, E. L. Heacock, W. A. Morgan, R. H. Moore, E. C. Mangold, and S. D. Soules, "Indirect Measurements of Atmospheric Temperature Profiles from Satellites: III. The Spectrometers and Experiments," *Monthly Weather Review*, vol. 94, No. 6, June 1966, pp. 367-377.
6. I. Holmström, "On a Method for Parametric Representation of the State of the Atmosphere," *Tellus*, vol. 15, No. 2, May 1963, pp. 127-149.
7. D. G. James, "Indirect Measurements of Atmospheric Temperature Profiles from Satellites: IV. Experiments with Phase 1 Satellite Infrared Spectrometer," *Monthly Weather Review*, vol. 95, No. 7, July 1967, pp. 457-462.
8. F. Saiedy, "Absolute Measurements of Infrared Radiation in the Atmosphere," Ph. D. Thesis, University of London, 1960.
9. D. Q. Wark, "On Indirect Temperature Soundings of the Stratosphere from Satellites," *Journal of Geophysical Research*, vol. 66, No. 1, Jan. 1961, pp. 77-82.
10. D. Q. Wark and H. E. Fleming, "Indirect Measurements of Atmospheric Temperature Profiles from Satellites: I. Introduction," *Monthly Weather Review*, vol. 94, No. 6, June 1966, pp. 351-362.
11. M. Wolk, F. Van Cleef, and G. Yamamoto, "Indirect Measurements of Atmospheric Temperature Profiles from Satellites: V. Atmospheric Soundings from Infrared Spectrometer Measurements at the Ground," *Monthly Weather Review*, vol. 95, No. 7, July 1967, pp. 463-467.